Genes & Diseases (2024) 11, 382–396

Available online at www.sciencedirect.com

ScienceDirect

journal homepage: www.keaipublishing.com/en/journals/genes-diseases

FULL LENGTH ARTICLE

RNA m^{6}A reader YTHDF2 facilitates precursor miR-126 maturation to promote acute myeloid leukemia progression

Zheng Zhang [a,b,1], Keren Zhou [a,1], Li Han [a,k], Andrew Small [a], Jianhuang Xue [a,j], Huilin Huang [a,d], Hengyou Weng [a,e,f], Rui Su [a], Brandon Tan [a], Chao Shen [a], Wei Li [a], Zhicong Zhao [a,g], Ying Qing [a], Xi Qin [a,b], Kitty Wang [a], Keith Leung [a], Mark Boldin [a], Chun-Wei Chen [a], David Ann [b,h], Zhijian Qian [i], Xiaolan Deng [a,*], Jianjun Chen [a,c,*], Zhenhua Chen [a,*]

[a] *Department of Systems Biology, Beckman Research Institute of City of Hope, Monrovia, CA 91016, USA*
[b] *Irell and Manella Graduate School of Biological Sciences, Beckman Research Institute of City of Hope, Duarte, CA 91010, USA*
[c] *Gehr Family Center for Leukemia Research, City of Hope, Duarte, CA 91010, USA*
[d] *Sun Yat-sen University Cancer Center, State Key Laboratory of Oncology in South China, Collaborative Innovation Center for Cancer Medicine, Guangzhou, Guangdong 510060, China*
[e] *Guangzhou Laboratory, Guangzhou, Guangdong 510005, China*
[f] *Bioland Laboratory, Guangzhou, Guangdong 51005, China*
[g] *Department of Liver Surgery, Renji Hospital, Shanghai Jiao Tong University School of Medicine, Shanghai 200127, China*
[h] *Department of Diabetes Complications and Metabolism, Beckman Research Institute of City of Hope, Duarte, CA 91010, USA*
[i] *Department of Biochemistry and Molecular Biology, University of Florida, Gainesville, FL 32603, USA*
[j] *Tongji Hospital Affiliated to Tongji University, Frontier Science Center for Stem Cell Research, School of Life Sciences and Technology, Tongji University, Shanghai 200092, China*
[k] *School of Pharmacy, China Medical University, Shenyang, Liaoning 110001, China*

Received 27 November 2022; received in revised form 16 January 2023; accepted 25 January 2023
Available online 28 March 2023

* Corresponding author. Department of Systems Biology, Beckman Research Institute of City of Hope, Monrovia, CA 91016, USA.
E-mail addresses: xideng@coh.org (X. Deng), jianchen@coh.org (J. Chen), zhenhchen@coh.org (Z. Chen).
Peer review under responsibility of Chongqing Medical University.
[1] These authors contributed to this work equally.

https://doi.org/10.1016/j.gendis.2023.01.016

KEYWORDS
AML;
miR-126;
N^6-methyladenosine;
Pre-miRNA maturation;
YTHDF2

Abstract As the most common internal modification of mRNA, N^6-methyladenosine (m^6A) and its regulators modulate gene expression and play critical roles in various biological and pathological processes including tumorigenesis. It was reported previously that m^6A methyltransferase (writer), methyltransferase-like 3 (METTL3) adds m^6A in primary microRNAs (pri-miRNAs) and facilitates its processing into precursor miRNAs (pre-miRNAs). However, it is unknown whether m^6A modification also plays a role in the maturation process of pre-miRNAs and (if so) whether such a function contributes to tumorigenesis. Here, we found that YTHDF2 is aberrantly overexpressed in acute myeloid leukemia (AML) patients, especially in relapsed patients, and plays an oncogenic role in AML. Moreover, YTHDF2 promotes expression of miR-126-3p (also known as miR-126, as it is the main product of precursor miR-126 (pre-miR-126)), a miRNA that was reported as an oncomiRNA in AML, through facilitating the processing of pre-miR-126 into mature miR-126. Mechanistically, YTHDF2 recognizes m^6A modification in pre-miR-126 and recruits AGO2, a regulator of pre-miRNA processing, to promote the maturation of pre-miR-126. *YTHDF2* positively and negatively correlates with miR-126 and miR-126's downstream target genes, respectively, in AML patients, and forced expression of miR-126 could largely rescue *YTHDF2*/*Ythdf2* depletion-mediated suppression on AML cell growth/proliferation and leukemogenesis, indicating that miR-126 is a functionally important target of YTHDF2 in AML. Overall, our studies not only reveal a previously unappreciated YTHDF2/miR-126 axis in AML and highlight the therapeutic potential of targeting this axis for AML treatment, but also suggest that m^6A plays a role in pre-miRNA processing that contributes to tumorigenesis.

Introduction

Gene expression is fine-tuned by chemical decorations of nucleic acids, the process of which is termed epigenetics (for DNA) and epitranscriptomics (for RNA).[1–3] As the most abundant internal chemical modification on messenger RNA (mRNA), N^6-methyladenodine (m^6A) is delicately regulated.[1,3] Co-transcriptionally, a methyl group is deposited to the N^6 position of adenosine in mRNAs or noncoding RNAs by the methyltransferase ("writer") complex containing METTL3, METTL14, and other regulatory subunits (WTAP, VIMIR, ZC3H13, etc.)[4–8] or by other writers such as METTL16 and ZCCHC4.[9–16] Conversely, m^6A can be removed from RNA substrates by demethylases (erasers) i.e., FTO and ALKBH5.[17,18] Functionally, selective recognition and binding of m^6A by the "reader" proteins in the nucleus (YTHDC1, HNRNPA2B1, HNRNPC, etc.) or the cytosol (YTHDF1-3, IGF2BP1-3, EIF3b, etc.) may affect splicing, nuclear retention, translation, and stability of the substrate mRNA.[3,19–26] Furthermore, m^6A can regulate the expression and function of non-coding RNAs including long non-coding RNA (lncRNA), circular RNA (circRNA), and microRNA (miRNA).[2,25,27,28]

MiRNAs are small non-coding RNAs (18—22 nucleotide long) that regulate gene expression post-transcriptionally.[29,30] MiRNAs may cause translation inhibition and/or degradation of their target mRNAs, which subsequently modulates various biological processes (development, differentiation, metabolism, etc.), and diseases (dementia, cancer, etc.).[29–35] In the hematopoietic system, miRNAs regulate both hematopoiesis and leukemogenesis.[30,36–38] Specifically, miRNAs have been reported to play critical roles in acute myeloid leukemia (AML) and represent potential therapeutic targets, while miRNA signatures can serve as biomarkers for diagnosis, classification and prognosis in AML.[30,36,38–44]

Numerous studies have identified m^6A-related genes as key regulators of AML initiation, progression, and drug resistance, and some also play important roles in normal hematopoiesis.[1,2,17,45–51] We and others have shown that both m^6A writers (METTL3/14) and erasers (FTO and ALKBH5), as well as several readers (e.g., YTHDF2, IGF2BP2 and YTHDC1) play oncogenic roles in AML.[17,18,45–48,52–57] Notably, depletion of YTHDF2 selectively inhibits AML progression and leukemia stem cell (LSC) self-renewal while promoting normal hematopoietic stem cell (HSC) expansion, making it an ideal candidate for treating AML.[46,58–60] However, the underlying molecular mechanism has yet to be fully investigated. YTHDF2 is a canonical m^6A reader known to promote the degradation of its target mRNA.[23] Interestingly, a recent study reported that YTHDF2 participates in METTL3-mediated promotion of the processing of pri-miR-150, which in turn promotes miR-150 expression and suppresses neuropathic pain, indicating a new role of YTHDF2 in the regulation of miRNA biogenesis.[61] Given the close connections among YTHDF2, AML, and miRNA, we wonder whether YTHDF2 regulates AML progression by modulating the expression of certain miRNA(s).

Here, we report that YTHDF2 promotes AML progression at least in part through post-transcriptionally enhancing the expression of miR-126 (i.e., miR-126-3p), a miRNA that has been reported to promote AML progression and LSC self-renewal, while its depletion also enhances HSC expansion.[37,62–67] YTHDF2 recognizes m^6A in the precursor miR-126 (pre-miR-126) as an m^6A reader and recruits AGO2 (a key protein for miRNA biogenesis) and thereby facilitates its maturation, which in turn promotes the expression of mature miR-126 and accelerates AML progression.

Material and methods

Database analysis

The expression of YTHDF2 in the healthy bone marrow and AML patients was analyzed using data obtained from Microarray Innovations in LEukemia (MILE) study and plotted on Bloodspot (https://servers.binf.ku.dk/bloodspot/).[68,69] Data for YTHDF2 expression in AML patients with or without bone marrow relapse was obtained from the Therapeutically Applicable Research to Generate Effective Treatments (TARGET) program and plotted on XenaBrowser.[70] Correlation between the expression of YTHDF2 and miR-126 or miR-15b was analyzed using data from The Cancer Genome Atlas (TCGA) and plotted on the Encyclopedia of RNA Interactomes (ENCORI).[71] Correlations of expression between YTHDF2 and multiple genes were analyzed using data from TCGA and plotted on ENCORI.[71]

Cell culture

MonoMac6 (MM6) was obtained from DSMZ and cultured in RPMI1640 (11875119, Thermo Fisher Scientific) supplemented with 10% FBS plus 2 mM L-glutamine (25030-081, Thermo Fisher Scientific), 1× non-essential amino acids (11140050, Gibco), 1 mM sodium pyruvate (11360070, Thermo Fisher Scientific), 10 μg/mL human insulin (12585014, Thermo Fisher Scientific). THP1, U937, C1498, and Molm13 were purchased from ATCC and cultured in RPMI1640 supplemented with 10% FBS and 1% penicillin/streptomycin; HEK293T was purchased from ATCC and cultured in cultured in DMEM supplemented with 10% FBS and 1% penicillin/streptomycin. All cells were maintained in a 37 °C, 5% CO_2 humidified incubator. Plasmocin prophylactic was supplemented in all media to prevent potential contamination.

Flow cytometry and apoptosis analysis

Flow cytometry was performed in the City of Hope core facility and data was analyzed with FlowJo. Briefly, for c-kit expression, cells were stained with anti-mouse CD45.2-PE (12-0454-83, Thermo Fisher Scientific) and anti-mouse c-kit-APC (17-1171-83, eBioscience) and analyzed on BD Fortessa Cell Analyzer following the manufacturer's directions. For data analysis, we gated for live, singlets, with positive CD45.2 expression to selectively focus on leukemic cells before analyzing for c-Kit expression. For apoptosis analysis, cells were stained with 7-AAD and Annexin V using the Annexin V Apoptosis Detection Kit (88-8007-74, eBioscience) and analyzed on BD Fortessa Cell Analyzer according to the manufacturer's instructions.

Primary AML patient and healthy donor specimens

Primary human AML patient samples were collected at the time of diagnosis, relapse, or remission after written informed consent at City of Hope Hospital (COH) or Cincinnati Children's Hospital Medical Center (CCHMC) in congruence with the protocol approved by the institutional review board (IRB). Samples were processed or maintained according to previously described methods.[45] Normal MNC, CD34+ hematopoietic stem/progenitor cells (HSPCs), and CD34-cells were purified from cord blood, bone marrow, or peripheral blood of healthy donors from CCHMC or COH.

Plasmids and shRNAs

The following plasmids were generated or used in our lab as described in our previous publications: MSCV-neo-MLL-AF9, MSCV-PIG-mir-Control, and MSCV-PIG-pre-miR-126. pLKO.1-shNS, shYTHDF2-1 (TRCN0000265510), shYTHDF2-2 (TRCN0000254411), PCDH-YTHDF2,.[17,19,45,65,72,73] For pmiRNA1-YTHDF2, we used PCDH-YTHDF2 as template, amplified YTHDF2 by PCR, then cut and ligated the PCR product into the pmiRNA1 lentiviral vector following published protocols.[45] For PCDH-AGO2 and pmiRNA1-AGO2, we used cDNA of 293T cells as template, amplified AGO2 by PCR, then cut and ligated the PCR product into PCDH or pmiRNA1 backbones.

Viral production and transduction

Detailed methods are described in our previous publications.[19,45] Briefly, retroviruses or lentiviruses were produced in 293T cells by co-transfection of an individual expression construct with the pCL-Eco packaging vector (IMGENEX, San Diego, CA) or the pMD2.G:pMDLg/pRRE:pRSV-Rev packaging mix (individually purchased from Addgene), respectively. The media was replaced 8 h post-transfection and the supernatant was filtered through a 0.45 μm syringe filter and then collected at 48- and 72-h post-transfection. The supernatants from both time points were pooled for transduction or concentrated with PEG-It (Systems Bioscience, LV825A-1) before being aliquoted and frozen at −80 °C until use. Media containing viruses was added to cells with 8 μg/mL polybrene (Sigma-Aldrich) and one or two rounds of spinoculation were performed for transduction. The media was replaced 24 h later and 2 μg/mL puromycin was added for selection if needed.

Animal experiments

Ythdf2$^{fl/fl}$ mice were generated in our lab as described in previous publications.[74] *Ythdf2*$^{fl/fl}$ mice were crossed to *Mx1-Cre* transgenic mice to generate *Ythdf2*$^{fl/fl}$*Mx1*-Cre mice. *Ythdf2* was conditionally knocked out after injecting Polyinosinic: polycytidylic acid (poly I:C) (428750 R&D Systems) i.p. at 300 μg each time per mice to *Ythdf2*$^{fl/fl}$*Mx*-Cre mice every other day for five times. NCI C57BL/6 mice were purchased from Charles River Laboratories. All mice were maintained according to the Institutional Animal Care and Use Committee (IACUC) protocols approved by City of Hope. All mice were housed on a 12 h:12 h, light:dark cycle with food and water ad libitum. Mice were randomly assigned to experimental groups.

Cell proliferation assay (MTT)

Cell proliferation was assessed using CellTiter 96® Non-Radioactive Cell Proliferation Assay (MTT, G400, Promega)

following the manufactures recommendations. Briefly, cells were seeded into 96-well plates (5000—10,000 cells per well). The dye solution with a volume of 15 μL was added to each well every 24 h and incubated at 37 °C for 2—4 h before 100 μL stop solution was added to quench the reaction. Finally, the absorbance at 570 nm was determined using a microplate reader the following day.

Colony-forming assay (CFA)

CFA was performed as described in our previous publications.[45] Briefly, cells were collected from bone marrow of CD45.2 *Ythdf2*$^{fl/fl}$*Mx1*-Cre mice, selected for lin-population using BMMNCs Lineage Cell Depletion Kit (130-090-858, Miltenyi Biotech), and transduced with MA9 retrovirus by spinoculation following afore mentioned protocol. ColonyGel 1201-mouse base medium (1201, Reachbio) were used for seeding cells at 20, 000 per 35 mm dish. Murine cytokines and reagents were supplemented as follows: 10 ng/mL of IL-3, IL-6, GM-CSF, 30 ng/mL of SCF, and 1 mg/mL of G418. Colonies were counted 6—7 days after plating. For CFA of human AML cell lines, cells were transduced with lentiviral shRNAs before seeded into ColonyGel 1101-human base medium (1101, Reachbio) supplemented with 2 μg/mL puromycin in 35 mm dishes at 20, 000 cells/dish. Colonies were observed daily and counted 6—7 days after plating.

Mouse bone marrow transplantation (BMT)

These assays were conducted as described previously with some modifications.[45,72] Briefly, cells were collected from the CD45.2 *Ythdf2*$^{fl/fl}$*Mx1*-Cre mice, enriched for lin-population, and transduced with retroviral MA9 alone or retroviral MA9 + MSCV-pre-miR-126/MSCV-pre-miR-Control by spinoculation as described before. Clonal cells from CFA assays were washed and suspended together with healthy mouse BM cells (0.5 million CFA cells + 1 million healthy BM per mouse) with ice-cold PBS, and subsequently injected via the tail vein into lethally (900 rads) irradiated 8 to 10-week-old B6.SJL (CD45.1) recipient mice. Ten days after the injection, knockout was induced by i.p. delivering of poly I:C (428750 R&D Systems) at 300 μg each time per mice every other day for five times. Mice were observed regularly after cell injection and samples were collected at the end point.

Western blotting

We followed published protocols.[45] Briefly, cells were counted, washed with ice-cold PBS, and lysed using 1× SDS buffer (100 mL for 1 × 10^6 cells). After being heated at 95 °C for 10 min, samples were loaded to and separated by 10% SDS-PAGE before being transferred to Polyvinylidene Fluoride (PVDF) membranes. Membranes were blocked with 5% non-fat milk (Bio-Rad), incubated sequentially with primary and secondary antibodies then detected with the Pierce ECL Western Blotting Substrate (Thermo Fisher Scientific) or Amersham ECL Prime Western Blotting Detection Reagent (GE Healthcare). Antibodies used for western blotting were as follows: YTHDF2 (24744-1-AP, Proteintech), AGO2 (MABE253, Sigma-Aldrich), GAPDH (sc-47724, Santa Cruz Biotechnology, Dallas, TX), β-Actin (3700, Cell SignalingTechnology). GAPDH or ACTB was used as a loading control. Protein quantification was performed by Image J and normalized to reference protein.

Co-immune precipitation

Cells were counted, washed in ice-cold PBS, and lysed in M-PER (78501, Thermo Fisher Scientific) supplemented with HaltTM protease and phosphatase inhibitors (Thermo Fisher Scientific) before sonicated (Qsonica Q800R) in cold water (60% amplification) for 20 min. The lysate was cleared by centrifugation before protein concentration was determined. A small amount of lysate was saved for input. The lysate was mixed with 50 μL protein A/G beads (Pierce 88803) and one of the pull-down antibodies: normal mouse IgG (NI03-100UG, Millipore); normal rabbit IgG (NI01-100UG, Millipore); FLAG antibody (F3165-5 MG, Sigma-Aldrich); YTHDF2 (24744-1-AP, Proteintech). The mixture was incubated at 4 °C overnight with rotation. Then the supernatant was discarded and the beads were washed with ice-cold lysis buffer 3 times before eluting with SDS buffer. The eluted samples were used for western blots as described.

RNA extraction and RT-qPCR

Total RNA was isolated using the TRIzol reagent (Thermo Fisher Scientific) and Direct-zol RNA miniprep kits (R2050, Zymo) according to the manufacturer's instructions. For cDNA synthesis, 200-1000 ng of total RNA was reverse-transcribed into cDNA in a total reaction volume of 10 μL with the QuantiTect Reverse Transcription kit (205314, QIAGEN) following the manufacturer's instructions. Quantitative real-time PCR (qPCR) was performed with Maxima SYBR Green qPCR Master Mix (2 ×) (FEPK0253, Thermo Fisher) on a QuantStudio (TM) 7Flex Real-Time PCR system (Applied Biosystem). ACTB or GAPDH was used as an internal control for gene expression evaluation. QPCR for miRNAs including the primary and precursor forms was performed following published methods using U6 as internal control.[75—77] All primer sequences are listed in Table S1.

Methylated RNA immunoprecipitation (meRIP)-qPCR

To determine m^{6}A modification in pre-miR-126, meRIP-qPCR was performed using Magana meRIP m^{6}A kit (17—10499, Millipore) according to the manufacture's instructions and previous reports.[18,19,45,78] Briefly, total RNA was extracted using TRIzol and Direct-zol RNA miniprep kits (R2050, Zymo) following the manufacturer's instructions. The 300 ug total RNA was used for each IP-sample and one tenth of RNA was saved as input control. RNA was incubated with anti-m^{6}A antibody or control mouse IgG antibody conjugated beads with rotation for 2 h at 4 °C. After washing 3 times with 1 × IP buffer, samples were eluted twice with m^{6}A elution buffer. The eluted samples were purified using RNA Clean & Concentrator-5 (R1013 Zymo). Input RNA and MeRIP-ed RNA were further analyzed by qPCR. The enrichment of m^{6}A in each sample was

calculated by normalizing Ct values of the IP samples to the Ct values of the corresponding input portion.

RNA immunoprecipitation (RIP)-qPCR

The RIP experiment was performed according to previous reports from our lab with some modifications.[79] Briefly, MM6 cells were collected, washed with ice-cold PBS and then lysed with 1 mL M-PER Mammalian Protein Extraction buffer (78501, Thermo Fisher Scientific) containing 1 × protease inhibitor (78438, Thermo Fisher Scientific) and 100 U/mL Ribolock RNase inhibitor (EO0382, Thermo Fisher Scientific). Samples were sonicated using Qsonica Q800R at 60% amplitude, 15 s on, 15 s off for 10 cycles before centrifuged at 12 000 rcf, 4 °C, for 10 min to collect the supernatant, 10% of which was saved as input. Protein A/G beads (Pierce 88803) were conjugated with antibodies targeting YTHDF2 (24744-1-AP, Proteintech) or normal rabbit IgG control (NI01-100UG, Millipore) before mixed with samples at 4 °C overnight. Beads were washed with RIP buffer (150 mM KCl, 25 mM Tris (pH 7.4), 5 mM EDTA, 0.5 mM DTT, 0.5% NP40, 100 U/mL RNase inhibitor) before treated with protease K and eluted with TRIzol and RNA Clean & Concentrator-5 (R1013 Zymo). The extracted RNA and input were analyzed by qPCR.

Statistical analyses

Statistical analyses of experimental data were calculated with Prism Version 8 (GraphPad Software). The log-rank test was used to determine the significance for survival plots. For comparison between two samples, the Student's *t*-test was employed. One-way ANOVA with Dunnett's test was used for comparisons between more than two samples. For the comparison of growth curves, Two-way ANOVA with Tukey's multiple comparisons test was used. *P*-values less than 0.05 were considered significant.

Results

YTHDF2 is overexpressed and plays a tumor-promoting role in AML

Using Bloodspot (https://servers.binf.ku.dk/bloodspot), we analyzed *YTHDF2* expression data in the Microarray Innovations in Leukemia (MILE) study and found that YTHDF2 RNA levels were significantly elevated in AML patient samples harboring various genetic mutations compared with healthy bone marrow (Fig. 1A). Furthermore, our Western blot results further confirmed that YTHDF2 was increased at the protein level in AML patient samples relative to healthy controls (Fig. 1B). Moreover, analysis of the GDC-TARGET-AML data set on the UCSC Xena browser (https://xenabrowser.net/) also showed that *YTHDF2* expression was higher in patients with bone marrow site relapse/induction failure compared with patients without (Fig. 1C).

Consistent with previous reports,[46,60] *YTHDF2* knockdown (KD) significantly inhibited the proliferation/growth and colony-formation of human AML cells, while promoting their apoptosis (Fig. 1D–I; Fig. S1A–D).

To further investigate the roles of Ythdf2 in leukemogenesis, we performed BM transplantation (BMT) using our in-house created *Ythdf2* conditional knockout (cKO) *Ythdf2*$^{fl/fl}$ *Mx1*-Cre; mice (Fig. S2A, B), coupled with a commonly used and highly aggressive AML model, i.e., MLL-AF9 (MA9)-induced AML,[17,18,45,57,80–87] different from the BMT AML models (including Hoxa9/Meis1-and MOZ-TIF2 (resulting from inv(8) (p11q13))-induced AML) used in the previous studies of YTHDF2 function in AML.[46] Briefly, we collected lineage negative (lin-) progenitor cells from BM of *Ythdf2*$^{fl/fl}$ *Mx1*-Cre mice, then transduced the cells with MLL-AF9 (MA9) retrovirus to induce leukemic transformation (Fig. 2A). Our *in vitro* colony-forming/replating assay (CFA) results showed that KO of *Ythdf2* significantly reduced the numbers and sizes of colonies formed by pre-leukemic cells indicating the functional importance of Ythdf2 for leukemic transformation (Fig. 2B–D; Fig. S2C). Furthermore, our BMT assays showed that conditionally induced KO of *Ythdf2* significantly inhibited MA9-induced leukemogenesis and prolonged overall survival in both primary and secondary BMT recipient mice (Fig. 2E–G; Fig. S2D). In addition, a significant decrease in spleen weight, white blood cell (WBC) counts, and c-kit + blast population was observed in the *Ythdf2* KO group relative to the control group (Fig. 2H; Fig. S2E). Overall, our results confirmed that Ythdf2 plays an oncogenic role in AML.

YTHDF2 regulates miR-126 expression

YTHDF2 is a canonical m^{6}A reader that typically targets mRNA.[23] Since m^{6}A modification and the associated machinery play a role in pri-miRNA maturation[25,27,61] and miRNAs play critical roles in AML,[30,36–40,62–67,87–91] we sought to investigate whether YTHDF2 functions through regulating miRNA maturation/expression in AML. First, we compared miRNAs regulated by METTL3 with miRNAs enriched in LSCs using data reported by other groups[27,36] and identified two candidate targets: miR-126 and miR-15b (Fig. 3A). Furthermore, data analysis using the TCGA database showed that the expression of miR-126 but not miR-15b positively correlates with the expression of *YTHDF2* in AML patients (Fig. 3B). Interestingly, since both miR-126 and YTHDF2 have been reported to be able to promote LSC self-renewal and AML progression, while suppressing normal HSC self-renewal and expansion,[37,46,58–60,62–67] miR-126 appears to be a promising target of YTHDF2 in AML. We then evaluated, in three different AML cell lines (MM6, MolM13, and U937), the effects of *YTHDF2* KD on miR-126 expression using qPCR. We observed that levels of miR-126 (i.e., miR-126-3p) but not its passenger strand miR-126-5p were significantly decreased upon *YTHDF2* KD (Fig. 3C, D; Fig. S3A–C). Furthermore, overexpression (OE) of *YTHDF2* increased miR-126 level (while slightly affecting miR-126-5p level) in both MolM13 and U937 cells (Fig. 3E, F; Fig. S3D). Additionally, in both primary and secondary BMT AML cells, KO of *Ythdf2* decreased the levels of murine miR-126a (homology of human miR-126) without significantly changing murine miR-126a-5p (Fig. 3G; Fig. S3E).

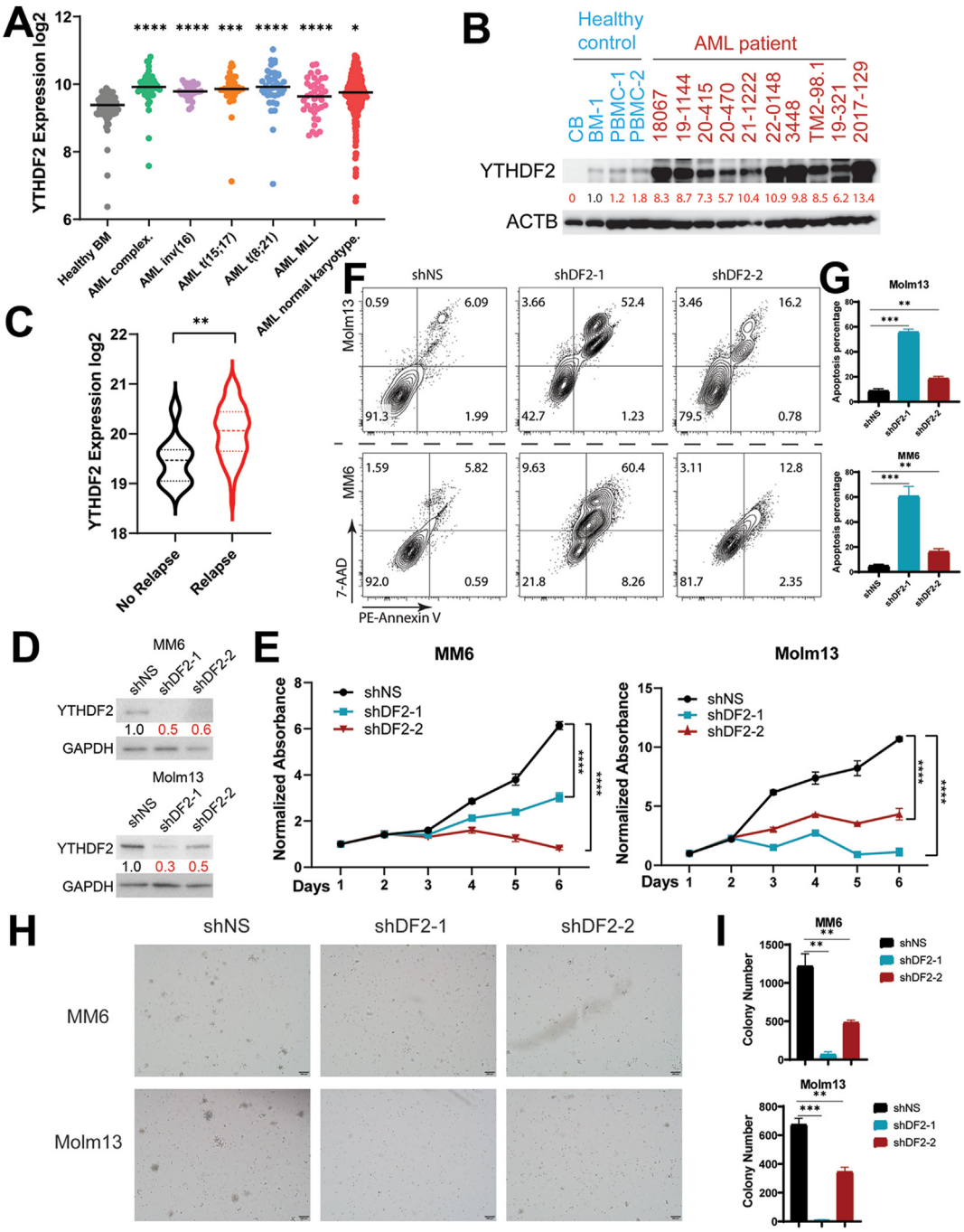

Figure 1 YTHDF2 is overexpressed in human AML and promotes AML cell growth/proliferation and colony-forming ability *in vitro*. **(A)** YTHDF2 expression in the healthy bone marrow (BM) and AML patients with different genetic backgrounds. AML MLL, *MLL*-rearranged AML. Data was obtained from MILE study and analyzed on Bloodspot (https://servers.binf.ku.dk/bloodspot/). *t*-test. *, $P < 0.05$; ***, $P < 0.001$; ****, $P < 0.0001$. **(B)** Western blot of YTHDF2 levels in AML patients and cord blood. (Quantification was analyzed by ImageJ and showing the ratios of YTHDF2 to ACTB, which were normalized to the value in the BM-1 sample.) (CB), BM, or peripheral blood mononuclear cell (PBMC) from healthy donors. **(C)** Expression of YTHDF2 in AML patients with or without relapse/induction failure. Data was obtained from TARGET and analyzed on Xena (https://xenabrowser.net/). *t*-test. **, $P < 0.01$. **(D)** Western blot showing KD efficiency of YTHDF2 in AML cell lines (MM6 (MONOMAC6) and Molm13). (Quantification was analyzed by ImageJ and showing the ratios of YTHDF2 to GAPDH. All groups were normalized to shNS.) **(E)** Growth/proliferation changes of MM6 and Molm13 cells upon *YTHDF2* KD as measured by MTT assay. Two-way Anova. ****, $P < 0.0001$. **(F, G)** Flow cytometry plots (F) and quantification (G) for apoptosis changes in MM6 and Molm13 cells upon YTHDF2 KD. **(H, I)** Numbers of colonies and representative pictures of colony-formation/replating assay (CFA) of MM6 and Molm13 cells with or without *YTHDF2* KD. *t*-test. **, $P < 0.01$; ***, $P < 0.001$.

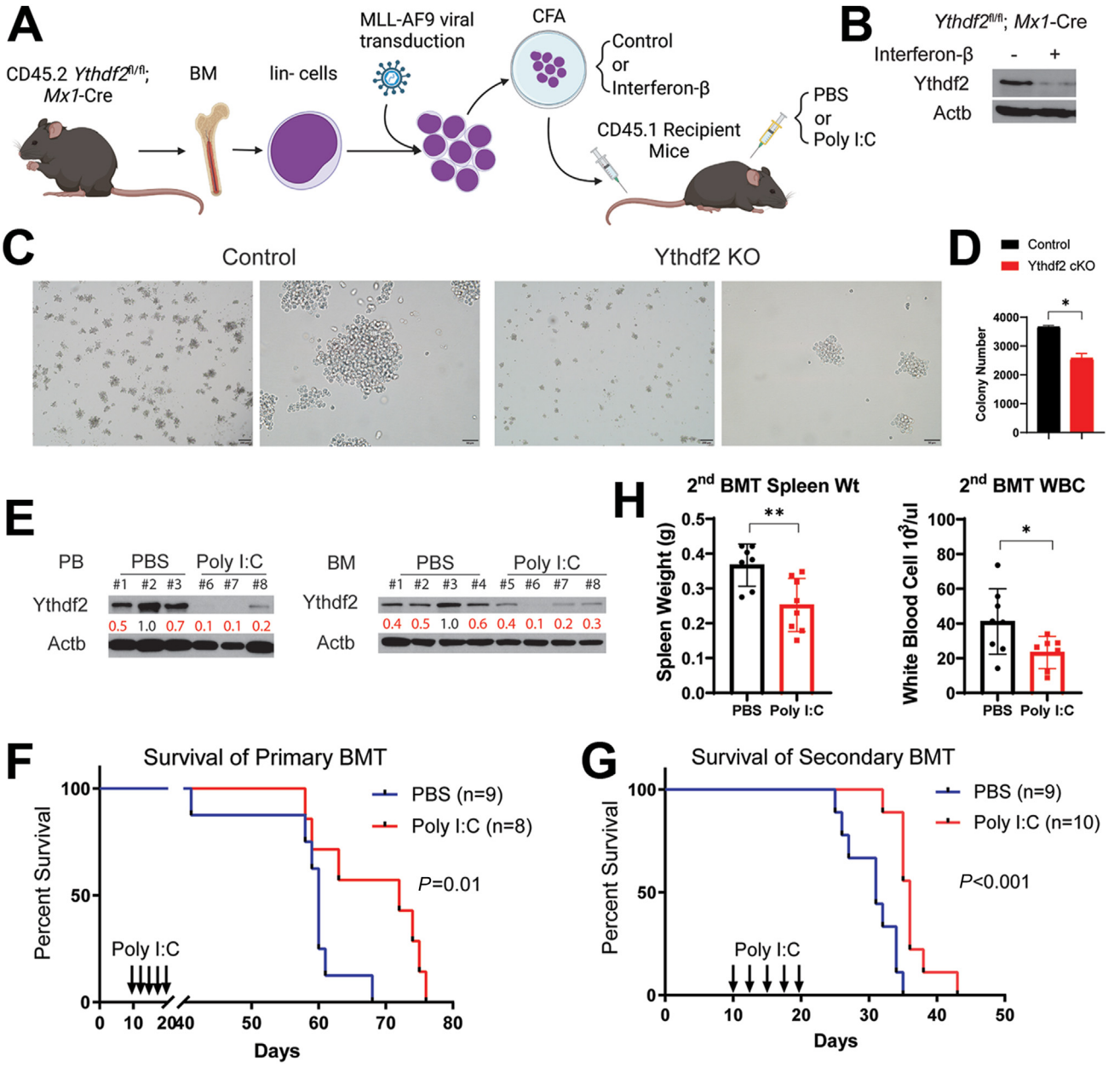

Figure 2 YTHDF2 facilitates leukemogenesis and progression of AML *in vivo*. **(A)** Schematic description for bone marrow transplantation (BMT) assay. Created with BioRender.com. **(B)** Western blot confirming *Ythdf2* conditional knockout (cKO) induced by interferon-β treatment. **(C, D)** Cells from *Ythdf2*$^{fl/fl}$; *Mx1*-Cre mice were treated with interferon-β to induce KO and treated with solvent of interferon-β as control. Representative pictures (C) and statistics (D) showing changes in the numbers and sizes of colonies in CFA after induced KO of Ythdf2. *t*-test. *, $P < 0.05$. **(E)** Western blot showing Ythdf2 protein level changes in PBMC and BM after *in vivo* KO induced by poly I:C injection. (Quantification was analyzed by ImageJ and showing the ratios of Ythdf2 to Actb. All samples were normalized to highest PBS sample.) **(F, G)** Kaplan-Meier survival curves of primary and secondary BMT recipient mice transplanted with leukemic cells with or without Ythdf2 cKO induced by poly I:C injection ($n = 8-10$ each group). Log-rank test. **(H)** Spleen weight and white blood cell (WBC) count of mice after secondary BMT with or without Ythdf2 cKO. *t*-test. *, $P < 0.05$; **, $P < 0.01$.

YTHDF2 interacts with AGO2 and facilitates pre-miR-126 processing

To illuminate the mechanism underlying the regulation of miR-126 expression by YTHDF2, we compared known regulators of miRNA biogenesis with potential YTHDF2 interacting partners identified by other groups using BioID,[92] and AGO2 stood out as the top candidate (Fig. 4A and Table S2). Our reciprocal co-IP data using MM6 and THP1 cells verified the interaction of YTHDF2 with AGO2 (Fig. 4B; Fig. S4A, B). Furthermore, we showed that KD of *YTHDF2* increased the levels of pre-miR-126 while decreasing the levels of mature miR-126 (Fig. 4C; Fig. S4C). Conversely, OE of *YTHDF2* decreased the level of pre-miR-126 and increased the

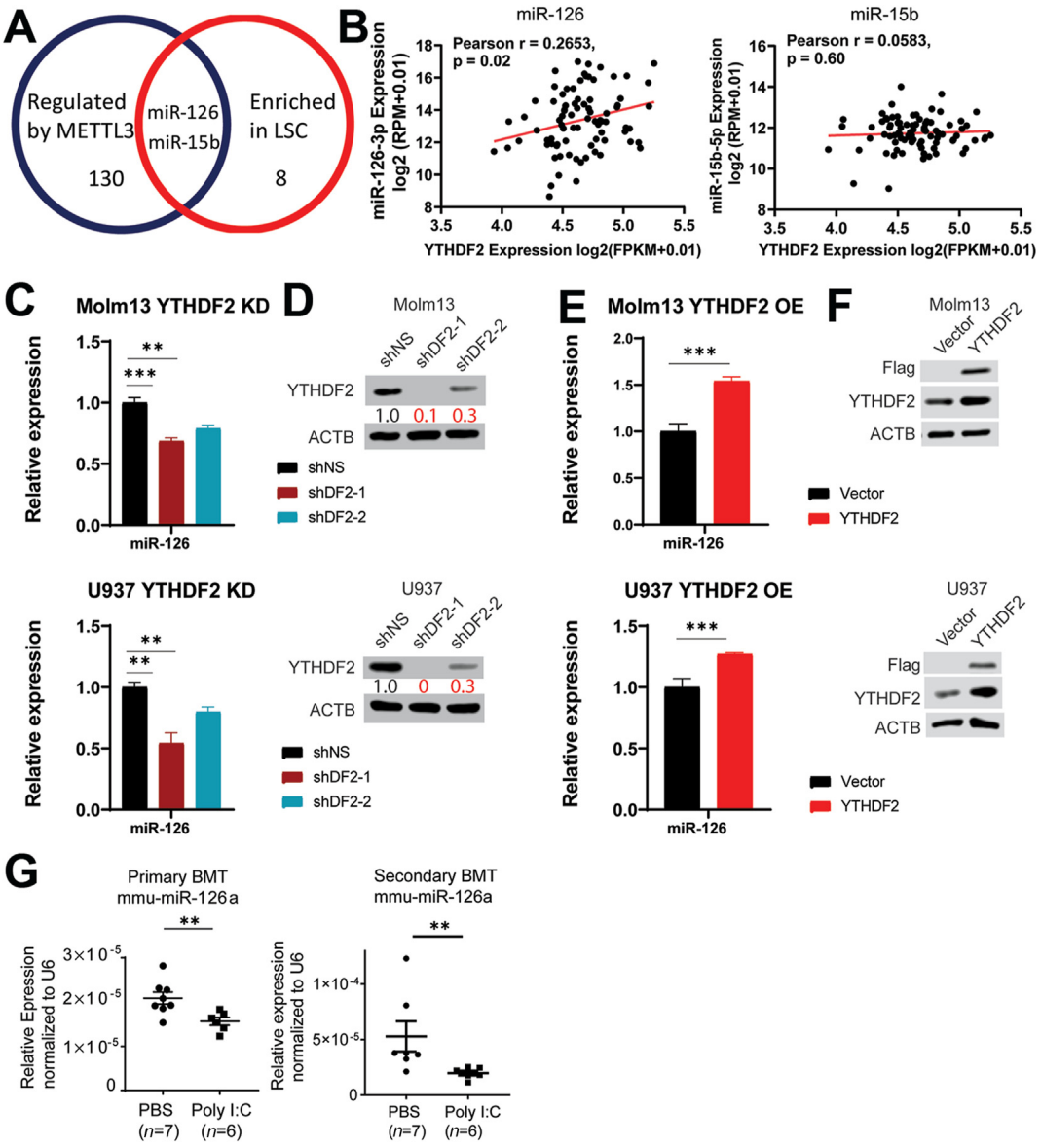

Figure 3 YTHDF2 regulates the expression of miR-126 in AML. **(A)** Analysis of published data showing overlapping of miRNAs regulated by METTL3 and miRNAs enriched in leukemic stem cells (LSCs).[27,36] **(B)** Correlation between expression of *YTHDF2* and expression of candidate miRNAs (miR-126 and miR-15b). Data was acquired from TCGA database and analyzed on ENCORI. Pearson correlation coefficient. **(C)** Level changes of miR-126 measured by qPCR in Molm13 and U937 cells after YT*HDF2* KD. *t*-test. **, $P < 0.01$; ***, $P < 0.001$. **(D)** Western blot showing KD efficiency of YTHDF2 by shRNAs in Molm13 and U937 cells. (Quantification was analyzed by ImageJ and showing the ratios of YTHDF2 to GAPDH. All groups were normalized to shNS.) **(E)** Level changes of miR-126 measured by qPCR in MolM13 and U937 cells after YTHDF2 OE. *t*-test. ***, $P < 0.001$. **(F)** OE of YTHDF2 validated by Western blot. **(G)** QPCR data showing miR-126a expression levels in MA9 transduced mice leukemia cells collected from BM of primary and secondary BMT recipient mice. *t*-test. **, $P < 0.01$.

expression level of miR-126 (Fig. 4D). Thus, our results suggest that YTHDF2 may regulate the processing of miR-126 from its precursor to mature form. To verify the association between m^{6}A modification and the regulation of pre-miR-126 processing by YTHDF2, we analyzed pre-miR-126 sequences from miRbase and found multiple m^{6}A motifs in both human and murine pre-miR-126 (Fig. 4E). In contrast, pre-miR-15b contains no m^{6}A motif (Fig. S4F), further suggesting that pre-miR-15b is not a direct target of YTHDF2. Our meRIP-qPCR data from MM6 cells confirmed m^{6}A modifications on pre-miR-126 (Fig. 4F). Moreover, induced KD of *METTL3* using lentiviral inducible shMETTL3-Tet1 in U937 cells decreased miR-126 and increased pre-miR-126 levels (Fig. 4G, H), suggesting that m^{6}A modification plays a role in pre-miR-126 maturation. In addition, our YTHDF2 RIP-qPCR data from MM6 cells demonstrated that YTHDF2 directly binds to pre-miR-126 (Fig. 4I). In MM6 and C1498 AML cells, forced expression of pre-miR-126 resulted in a substantial increase (over 100 folds) of mature miR-126 in expression, but KD of *YTHDF2* significantly attenuated

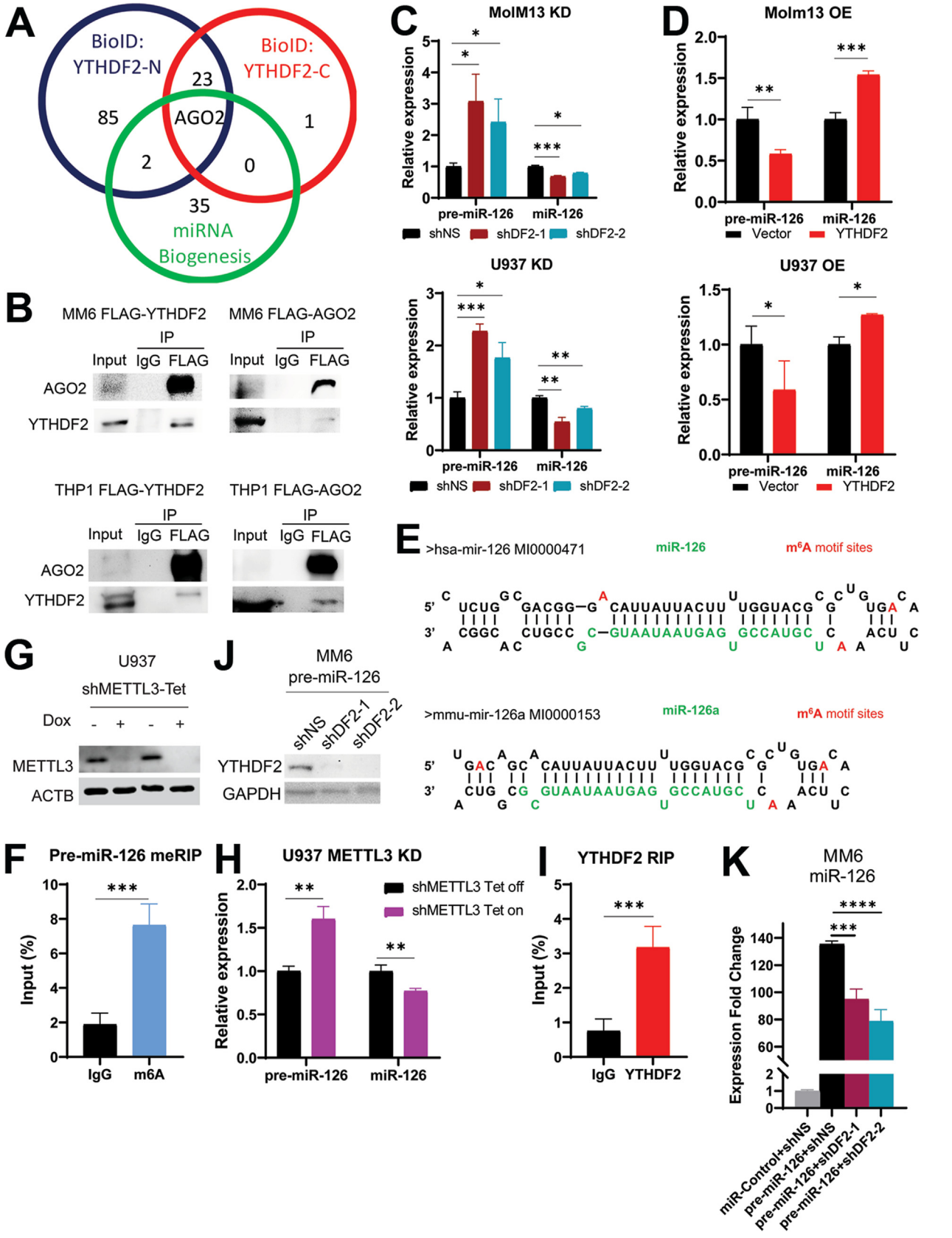

Figure 4 YTHDF2 interacts with AGO2 and facilitates pre-mir-126 processing. **(A)** Overlapping of miRNA biogenesis regulators and potential YTHDF2 interacting partners identified by BioID of YTHDF2 N-terminus and C-terminus (data from a study published by J.Y. Youn et al).[92] **(B)** Reciprocal co-IP between AGO2 and YTHDF2 using FLAG or control IgG antibodies in FLAG-tagged AGO2 or FLAG-tagged YTHDF2 overexpressing MM6 and THP1 cells. **(C)** Expression level changes of precursor and mature miR-126 after

this increase, further confirming that YTHDF2 regulates the processing of pre-miR-126 to its mature forms (Fig. 4J, K; Fig. S4D, E).

MiR-126 is a functionally important target of YTHDF2 in AML

To determine whether miR-126 is a functionally important target of YTHDF2 in AML, we performed rescue experiments by overexpressing miR-126 using miR-126 mimics after *YTHDF2* KD. First, we tested the OE efficiency of miR-126-3p mimics using qPCR and observed substantially elevated expression of miR-126 up to 7 days after transfection in MM6 cells (Fig. 5A). Our MTT assay data showed that OE of miR-126 promoted human AML cell proliferation/growth (Fig. 5B). Then, we overexpressed miR-126 in the MM6 cells with or without *YTHDF2* KD and observed that the cell growth inhibition caused by *YTHDF2* KD could be largely rescued by miR-126 OE (Fig. 5C, D). Furthermore, we performed BMT *in vivo* rescue experiment by overexpressing retroviral miR-126 in MA9-transformed *Ythdf2*$^{fl/fl}$ *Mx1*-Cre BM cells. As expected, OE of miR-126 could largely reversed the delayed AML onset and the prolonged survival caused by *Ythdf2* cKO in BMT recipient mice (Fig. 5E).

The YTHDF2/miR-126 axis regulates expression of downstream targets in AML

We next examined the effects of miR-126 OE and YTHDF2 KD on the expression of reported miR-126 down-stream target genes in AML,[36] and found that expression levels of multiple downstream targets (*ADAM9, ILK*, and *CDK3*) were significantly decreased by miR-126 OE and elevated by *YTHDF2* KD, while miR-126 OE largely reversed *YTHDF2* KD-mediated upregulation of these genes (Fig. 6A). In addition, analysis of the TCGA datasets at ENCORI[36,71] showed negative correlations between the expression of *YTHDF2* and that of miR-126 downstream targets in AML patient samples (Fig. 6B). Taken together, our data indicate that YTHDF2 facilitates the loading of pre-miR-126 to AGO2, an essential component of the miRNA Loading Complex (miRLC) and promotes the processing of pre-miR-126 to its mature form, hence displays an oncogenic role in AML.

Discussion

Characterized by the fast expansion of clonal, proliferative, and abnormally differentiated hematopoietic stem/progenitor cells, AML can be life-threatening without proper treatment.[93] Despite with improved risk stratification and therapeutics over the past decades, the 5-year overall survival rate for AML patients remains $< 30\%$.[93,94] Therefore, it is of great need for a better understanding of the mechanism underlying AML progression and thus coming up with a potential cure. Here, our *in vitro* and *in vivo* data indicate that YTHDF2 exhibits an oncogenic role in AML.[46,60] Albeit the treatment of poly I:C has been reported to affect hematopoiesis and/or leukemogenesis,[95,96] our results are highly consistent with those reported in the previous studies that employed genetic knockdown of *YTHDF2* to study the role of YTHDF2 in human AML progression in mouse models,[46,60] and all the results suggest that the suppression of AML progression *in vivo* after *Ythdf2*/*YTHDF2* KO/KD is most likely due to the loss of the oncogenic role of Ythdf2/YTHDF2. Different from the previous study reporting that Ythdf2 modulates *Tnfrsf1b* mRNA stability to promote AML progression,[46] here we revealed a distinct and novel mechanism by which YTHDF2 facilitates the maturation process of pre-miR-126, and thereby silences the miR-126 targets and promotes AML progression. Functionally, both miR-126 and YTHDF2 play dichotomous roles in LSCs and normal HSCs.[36,37,46,58,59,65] Specifically, depletion of either miR-126 or YTHDF2 hinders leukemia progression and LSC self-renewal while promoting normal HSC expansion.[36,46] Despite the largely overlapping downstream targets of miR-126 in LSCs and HSCs, some of the targets may function differently in LSCs and HSCs, which could potentially lead to the distinct roles of the YTHDF2/miR-126 axis in LSCs and HSCs.[36,62,97] One such target gene is *PTEN*.[97] Although not frequently mutated in AML, PTEN deficiency inhibits the maintenance of HSCs while promoting the expansion of LSCs.[97] Nevertheless, to further substantiate the molecular mechanism(s), future studies are warranted. These data and our functional rescue assay results all suggest that miR-126 is a crucial target of YTHDF2 in AML (and likely also in normal HSCs).

Ever since Alarcon et al. identified m^{6}A as an important regulator of miRNA biogenesis, extensive evidence has revealed that m^{6}A functions through miRNAs.[61,98–100] For instance, METTL14 displays an oncosupressor role in liver cancer by modulation of pri-miR-126 processing; METTL3 moderates the maturation of pri-miR-221/222 to promote bladder cancer proliferation; ALKBH5 regulates miR-192 expression and suppresses progression of esophageal cancer progression.[100–102] METTL3 coordinates with YTHDF2 to facilitate pri-miR-150 processing to regulate miR-150 expression[61] Strikingly, different from the previous studies that showed m^{6}A and the associated machinery facilitate the processing of pri-miRNAs, here we show for the first time that YTHDF2 facilitates the maturation of pre-miR-

YTHDF2 KD in MolM13 and U937 measured by qPCR. *t*-test. *, $P < 0.05$; **, $P < 0.01$; ***, $P < 0.001$. **(D)** Expression level changes of precursor and mature miR-126 after *YTHDF2* OE in MolM13 and U937. *t*-test. *, $P < 0.05$; **, $P < 0.01$; ***, $P < 0.001$. **(E)** Illustration of m^{6}A motifs on pre-miR-126 of humans and mice (potential methylation sites highlighted in red). Data sources: miRbase (https://www.mirbase.org/).[75] **(F)** m^{6}A-qPCR of pre-miR-126 in MM6 cells using IgG as control. *t*-test. ***, $P < 0.001$. **(G)** Inducible KD of lentiviral shMETTL3-Tet1 in U937 cells measured by western blots after doxycycline (Dox) induction. **(H)** Level changes of precursor and mature miR-126 after *METTL3* KD in U937 measured by qPCR. *t*-test. *, $P < 0.05$; **, $P < 0.01$; ***, $P < 0.001$; ****, $P < 0.0001$. **(I)** YTHDF2-RIP-qPCR analysis showing YTHDF2 directly binding to pre-miR-126 in MM6 cells. *t*-test. ***, $P < 0.001$. **(J)** Western blot of YTHDF2 in pre-miR-126 retroviral transduced MM6 cells with or without YTHDF2 KD. **(K)** Level changes of miR-126 in MM6 cells after pre-miR-126 retroviral transduction with or without *YTHDF2* KD. *t*-test. ***, $P < 0.001$; ****, $P < 0.0001$.

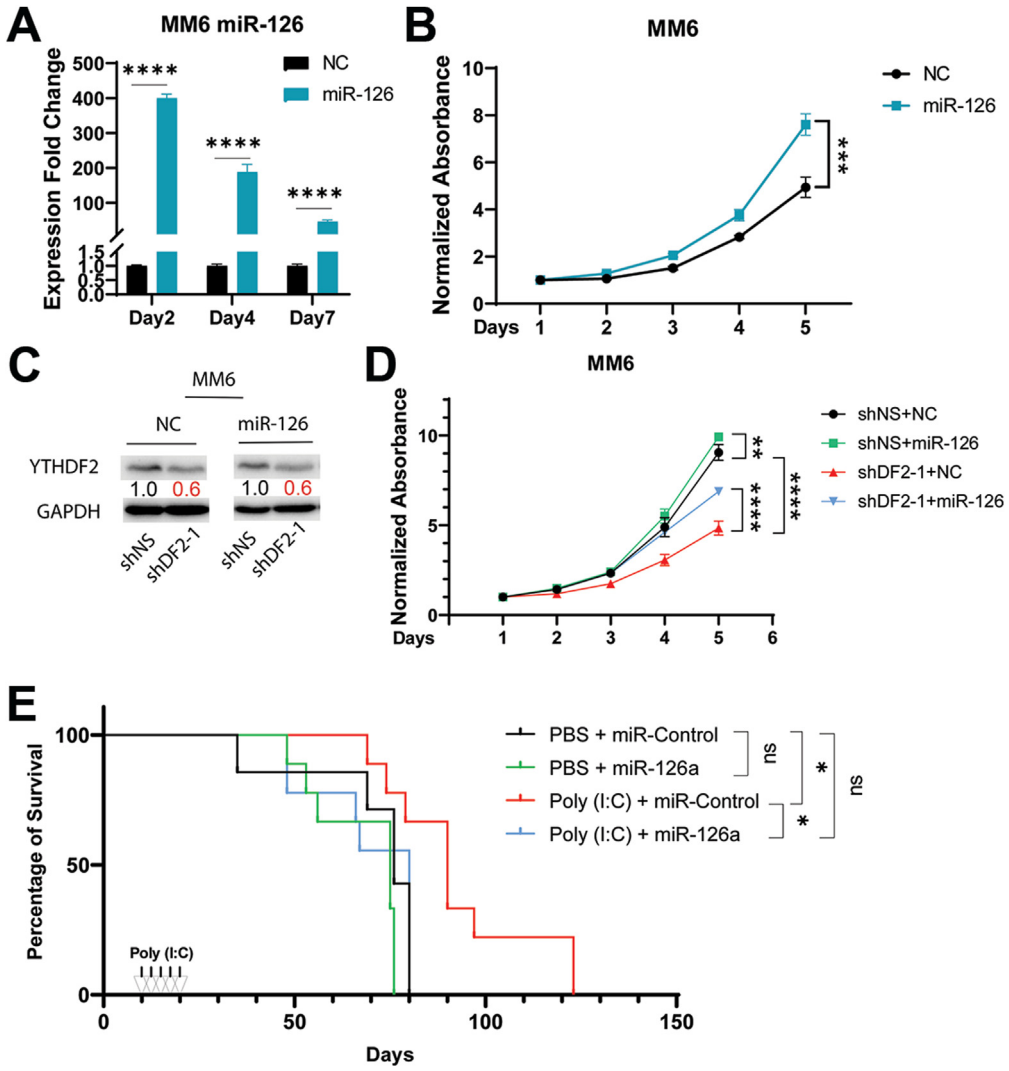

Figure 5 MiR-126 OE partially rescues growth inhibition induced by *YTHDF2* KD. **(A)** Levels of miR-126 on three time points (two, four, and seven days) after transfection of miR-126 mimics or negative control (NC) in MM6 cells. *t*-test. ****, $P < 0.0001$. **(B)** Growth changes of MM6 cells after miR-126 mimics transfection as measured by MTT. Two-way Anova. *t*-test. ***, $P < 0.001$. **(C)** Western blot of YTHDF2 in MM6 cells with or without *YTHDF2* KD and/or miR-126 OE. (Quantification was analyzed by ImageJ and showing the ratios of YTHDF2 to GAPDH. All groups were normalized to shNS.) **(D)** Growth changes (as measured by MTT) of MM6 cells after YTHDF2 KD with transfection of miR-126 mimics or NC. Two-way Aanova. **, $P < 0.01$; ****, $P < 0.0001$. **(E)** Kaplan-Meier survival curves for BMT recipient mice transplanted with MA9 leukemic cells with or without miR-126 OE rescue after Ythdf2 cKO induced by poly I:C injection ($n = 8$—10 each group). Log-rank test. NS = not significant; *, $P < 0.05$.

126. Indeed, whereas pri-miRNA processing typically takes place in the nucleus, pre-miRNA processing occurs in cytoplasm, which is consistent with YTHDF2's predominant distribution in the cytosol.[23,31] Therefore, our study unveiled another layer of m^{6}A fine-tuning miRNA biogenesis that m^{6}A and the associated machinery control pre-miRNA maturation processing.

YTHDF2 carries out its function through interacting with other proteins.[23,103] For example, YTHDF2 interacts with CCR4-NOT and causes degradation of its target mRNAs.[103] Here we show that YTHDF2 recruits AGO2 to facilitate the maturation process of pre-miR-126. As an essential part of both the RNA induced silencing complex (RISC) and the miRNA loading complex (miRLC), AGO2 modulates the processing of certain pre-miRNAs to their mature forms.[104,105] In addition, AGO2 is the only argonaute protein with nuclease activities for Dicer-independent miRNA such as miR-451.[104] Our reciprocal co-IP in two AML cell lines confirmed the interaction between AGO2 and YTHDF2 in AML cells. Furthermore, the interaction between YTHDF2 and AGO2 was also observed in lung cancer cells,[106] suggesting that YTHDF2 together with AGO2 may regulate pre-miRNA maturation process under various cellular settings. Previously, Frohn et al reported that YTHDF2 shows a weak preference for binding with AGO2 in the presence of mRNAs.[107] Since both AGO2 and YTHDF2 are mRNA binding proteins, binding to the same target(s) would likely enhance their interaction. Interestingly, this interaction, though weakened, was still observed after RNase treatment indicating a direct interaction between YTHDF2 and

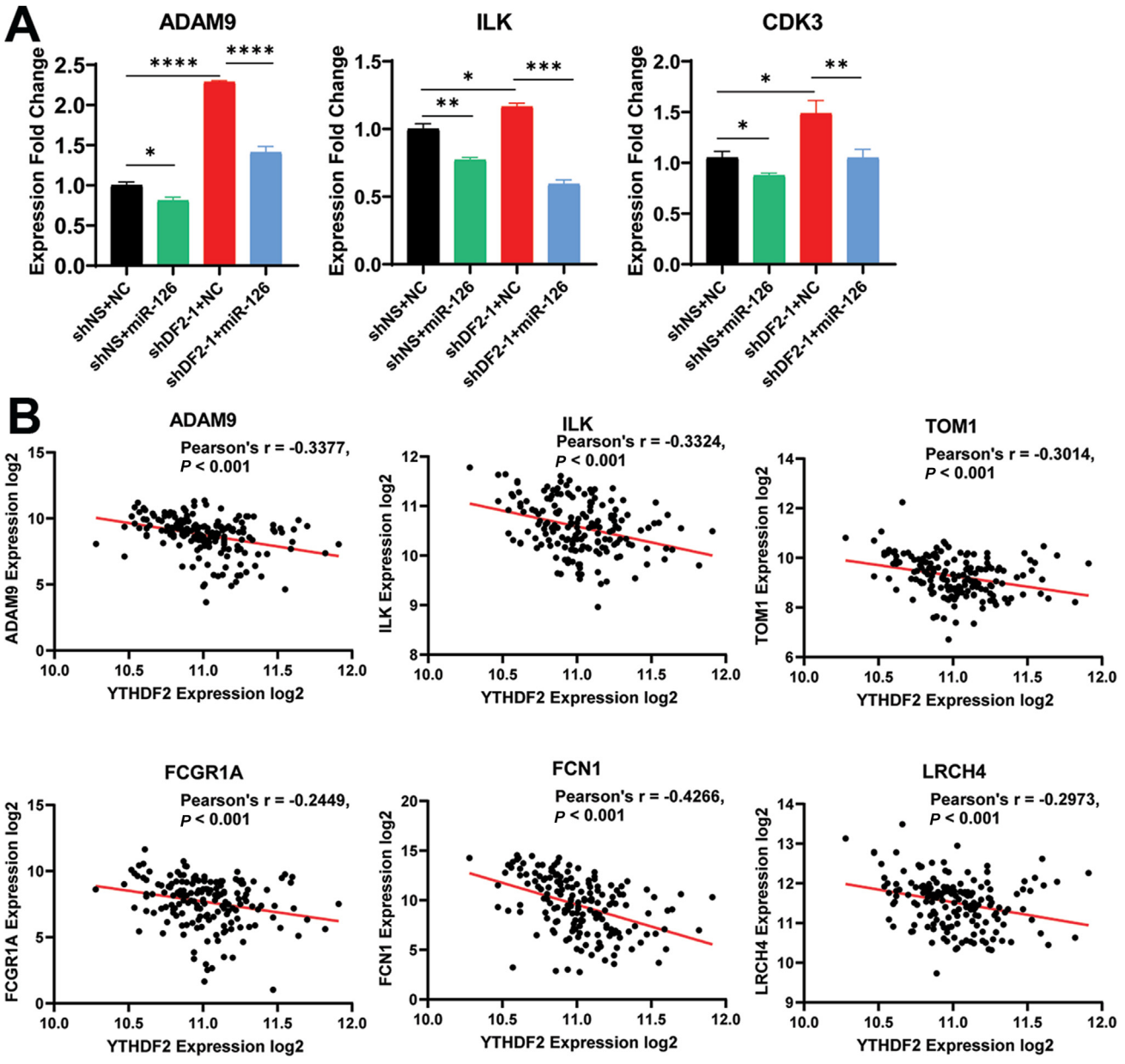

Figure 6 Downstream targets regulated by the YTHDF2/miR-126 axis in human AML. **(A)** QPCR showing expression changes of representative downstream target genes of miR-126 [36] in MM6 cells after miR-126 OE with or without YTHDF2 KD. *t*-test. *, $P < 0.05$; **, $P < 0.01$; ***, $P < 0.001$; ****, $P < 0.0001$. **(B)** Correlation between expression of reported miR-126 downstream target genes (*ADAM9*, *ILK*, *TOM1*, *FCGR1A*, *FCN1*, and *LRCH4*) and expression of *YTHDF2* in AML patients. Data acquired from TCGA and analyzed at Xena. r, Pearson correlation coefficient.

AGO2.[107] In the future, it would be interesting to explore whether the processing of other pre-miRNAs is also regulated by YTHDF2.

Conclusions

In summary, our studies uncover a novel function of YTHDF2 in regulating the processing of pre-miR-126 in an m^{6}A- and AGO2-dependent manner, which in turn enhances miR-126 expression and promotes AML progression. Our work together with previous studies also highlight the therapeutic potential of targeting the YTHDF2/miR-126 axis for AML treatment, which will selectively eradicate LSCs while enhancing the expansion of normal HSC population.

Author contributions

Z.Zhang, X.D., J.C., and Z.C.: Conceptualization, Project administration, and Supervision; Z.Zhang, L.H., A.S., K.W., K.L., X.D., and Z.C.: Investigation, Methodology, and Data curation; K.Z.: Data curation and Formal analysis; J.X. H.H., H.W., R.S., B.T., C.S., W.L., Z.Zhao., Y.Q., X.Q., M.B., C.C., D.A., Z.Q., X.D., J.C., and Z.C.: Resources, Funding acquisition, and Writing-editing; Z.Zhang, X.D., J.C., and Z.C.:

Writing-original draft, review and editing. All authors discussed the results and commented on the manuscript.

Conflict of interests

J.C. is a scientific advisory board member of Race Oncology. The other authors declare no potential conflict of interests.

Funding

This work was supported in part by the U.S. National Institutes of Health (NIH) grants R01 CA243386 (J.C.), R01 CA271497, R01 CA214965 (J.C.), R01 CA236399 (J.C.), R01 DK124116 (J.C), and The Simms/Mann Family Foundation (J.C.). J.C. is a Leukemia & Lymphoma Society (LLS) Scholar and is supported by the LLS 2022 Scholar CDP Achievement Award.

Appendix A. Supplementary data

Supplementary data to this article can be found online at https://doi.org/10.1016/j.gendis.2023.01.016.

References

1. Deng X, Su R, Weng H, Huang H, Li Z, Chen J. RNA N(6)-methyladenosine modification in cancers: current status and perspectives. *Cell Res*. 2018;28(5):507—517.
2. Huang H, Weng H, Chen J. m(6)A modification in coding and non-coding RNAs: roles and therapeutic implications in cancer. *Cancer Cell*. 2020;37(3):270—288.
3. Shi H, Wei J, He C. Where, when, and how: context-dependent functions of RNA methylation writers, readers, and erasers. *Mol Cell*. 2019;74(4):640—650.
4. Liu J, Yue Y, Han D, et al. A METTL3-METTL14 complex mediates mammalian nuclear RNA N6-adenosine methylation. *Nat Chem Biol*. 2014;10(2):93—95.
5. Wang P, Doxtader KA, Nam Y. Structural basis for cooperative function of Mettl3 and Mettl14 methyltransferases. *Mol Cell*. 2016;63(2):306—317.
6. Wen J, Lv R, Ma H, et al. Zc3h13 regulates nuclear RNA m(6)A methylation and mouse embryonic stem cell self-renewal. *Mol Cell*. 2018;69(6):1028—1038.e6.
7. Yue Y, Liu J, Cui X, et al. VIRMA mediates preferential m(6)A mRNA methylation in 3'UTR and near stop codon and associates with alternative polyadenylation. *Cell Discov*. 2018;4:10.
8. Scholler E, Weichmann F, Treiber T, et al. Interactions, localization, and phosphorylation of the m(6)A generating METTL3-METTL14-WTAP complex. *RNA*. 2018;24(4):499—512.
9. Brown JA, Kinzig CG, DeGregorio SJ, Steitz JA. Methyltransferase-like protein 16 binds the 3'-terminal triple helix of MALAT1 long noncoding RNA. *Proc Natl Acad Sci U S A*. 2016;113(49):14013—14018.
10. Pendleton KE, Chen B, Liu K, et al. The U6 snRNA m(6)A methyltransferase METTL16 regulates SAM synthetase intron retention. *Cell*. 2017;169(5):824—835.e14.
11. Warda AS, Kretschmer J, Hackert P, et al. Human METTL16 is a N(6)-methyladenosine (m(6)A) methyltransferase that targets pre-mRNAs and various non-coding RNAs. *EMBO Rep*. 2017;18(11):2004—2014.
12. Shima H, Matsumoto M, Ishigami Y, et al. S-adenosylmethionine synthesis is regulated by selective N(6)-adenosine methylation and mRNA degradation involving METTL16 and YTHDC1. *Cell Rep*. 2017;21(12):3354—3363.
13. Mendel M, Chen KM, Homolka D, et al. Methylation of structured RNA by the m(6)A writer METTL16 is essential for mouse embryonic development. *Mol Cell*. 2018;71(6):986—1000.e11.
14. Doxtader KA, Wang P, Scarborough AM, Seo D, Conrad NK, Nam Y. Structural basis for regulation of METTL16, an S-adenosylmethionine homeostasis factor. *Mol Cell*. 2018;71(6):1001—1011.e4.
15. Su R, Dong L, Li Y, et al. METTL16 exerts an m(6)A-independent function to facilitate translation and tumorigenesis. *Nat Cell Biol*. 2022;24(2):205—216.
16. Ma H, Wang X, Cai J, et al. N(6-)Methyladenosine methyltransferase ZCCHC4 mediates ribosomal RNA methylation. *Nat Chem Biol*. 2019;15(1):88—94.
17. Su R, Dong L, Li C, et al. R-2HG exhibits anti-tumor activity by targeting FTO/m(6)A/MYC/CEBPA signaling. *Cell*. 2018;172(1—2):90—105.e23.
18. Shen C, Sheng Y, Zhu AC, et al. RNA demethylase ALKBH5 selectively promotes tumorigenesis and cancer stem cell self-renewal in acute myeloid leukemia. *Cell Stem Cell*. 2020;27(1):64—80.e9.
19. Huang H, Weng H, Sun W, et al. Recognition of RNA N(6)-methyladenosine by IGF2BP proteins enhances mRNA stability and translation. *Nat Cell Biol*. 2018;20(3):285—295.
20. Han D, Liu J, Chen C, et al. Anti-tumour immunity controlled through mRNA m(6)A methylation and YTHDF1 in dendritic cells. *Nature*. 2019;566(7743):270—274.
21. Wang X, Zhao BS, Roundtree IA, et al. N(6)-methyladenosine modulates messenger RNA translation efficiency. *Cell*. 2015;161(6):1388—1399.
22. Shi H, Wang X, Lu Z, et al. YTHDF3 facilitates translation and decay of N(6)-methyladenosine-modified RNA. *Cell Res*. 2017;27(3):315—328.
23. Wang X, Lu Z, Gomez A, et al. N6-methyladenosine-dependent regulation of messenger RNA stability. *Nature*. 2014;505(7481):117—120.
24. Zhen D, Wu Y, Zhang Y, et al. m(6)A reader: epitranscriptome target prediction and functional characterization of N (6)-methyladenosine (m(6)A) readers. *Front Cell Dev Biol*. 2020;8:741.
25. Alarcon CR, Goodarzi H, Lee H, Liu X, Tavazoie S, Tavazoie SF. HNRNPA2B1 is a mediator of m(6)a-dependent nuclear RNA processing events. *Cell*. 2015;162(6):1299—1308.
26. Liu N, Dai Q, Zheng G, He C, Parisien M, Pan T. N(6)-methyladenosine-dependent RNA structural switches regulate RNA-protein interactions. *Nature*. 2015;518(7540):560—564.
27. Alarcon CR, Lee H, Goodarzi H, Halberg N, Tavazoie SF. N6-methyladenosine marks primary microRNAs for processing. *Nature*. 2015;519(7544):482—485.
28. Patil DP, Chen CK, Pickering BF, et al. m(6)A RNA methylation promotes XIST-mediated transcriptional repression. *Nature*. 2016;537(7620):369—373.
29. Gebert LFR, MacRae IJ. Regulation of microRNA function in animals. *Nat Rev Mol Cell Biol*. 2019;20(1):21—37.
30. Yendamuri S, Calin GA. The role of microRNA in human leukemia: a review. *Leukemia*. 2009;23(7):1257—1263.
31. Ha M, Kim VN. Regulation of microRNA biogenesis. *Nat Rev Mol Cell Biol*. 2014;15(8):509—524.
32. Wallace JA, O'Connell RM. MicroRNAs and acute myeloid leukemia: therapeutic implications and emerging concepts. *Blood*. 2017;130(11):1290—1301.
33. Ivey KN, Srivastava D. microRNAs as developmental regulators. *Cold Spring Harbor Perspect Biol*. 2015;7(7):a008144.
34. Cheng C, Li W, Zhang Z, et al. MicroRNA-144 is regulated by activator protein-1 (AP-1) and decreases expression of Alzheimer disease-related a disintegrin and metalloprotease 10 (ADAM10). *J Biol Chem*. 2013;288(19):13748—13761.

35. Rottiers V, Naar AM. MicroRNAs in metabolism and metabolic disorders. *Nat Rev Mol Cell Biol*. 2012;13(4):239—250.
36. Lechman ER, Gentner B, Ng SW, et al. miR-126 regulates distinct self-renewal outcomes in normal and malignant hematopoietic stem cells. *Cancer Cell*. 2016;29(2):214—228.
37. Zhang B, Nguyen LXT, Li L, et al. Bone marrow niche trafficking of miR-126 controls the self-renewal of leukemia stem cells in chronic myelogenous leukemia. *Nat Med*. 2018;24(4):450—462.
38. Chen J, Odenike O, Rowley JD. Leukaemogenesis: more than mutant genes. *Nat Rev Cancer*. 2010;10(1):23—36.
39. Li Z, Lu J, Sun M, et al. Distinct microRNA expression profiles in acute myeloid leukemia with common translocations. *Proc Natl Acad Sci U S A*. 2008;105(40):15535—15540.
40. Mi S, Lu J, Sun M, et al. MicroRNA expression signatures accurately discriminate acute lymphoblastic leukemia from acute myeloid leukemia. *Proc Natl Acad Sci U S A*. 2007;104(50):19971—19976.
41. Jiang X, Bugno J, Hu C, et al. Eradication of acute myeloid leukemia with FLT3 ligand-targeted miR-150 nanoparticles. *Cancer Res*. 2016;76(15):4470—4480.
42. Li Z, Huang H, Chen P, et al. miR-196b directly targets both HOXA9/MEIS1 oncogenes and FAS tumour suppressor in MLL-rearranged leukaemia. *Nat Commun*. 2012;3:688.
43. Fletcher D, Brown E, Javadala J, Uysal-Onganer P, Guinn BA. microRNA expression in acute myeloid leukaemia: new targets for therapy? *EJHaem*. 2022;3(3):596—608.
44. Bhatnagar B, Garzon R. Clinical applications of MicroRNAs in acute myeloid leukemia: a mini-review. *Front Oncol*. 2021;11:679022.
45. Weng H, Huang H, Wu H, et al. METTL14 inhibits hematopoietic stem/progenitor differentiation and promotes leukemogenesis via mRNA m(6)A modification. *Cell Stem Cell*. 2018;22(2):191—205.e9.
46. Paris J, Morgan M, Campos J, et al. Targeting the RNA m(6)A reader YTHDF2 selectively compromises cancer stem cells in acute myeloid leukemia. *Cell Stem Cell*. 2019;25(1):137—148.e6.
47. Cheng Y, Xie W, Pickering BF, et al. N(6)-Methyladenosine on mRNA facilitates a phase-separated nuclear body that suppresses myeloid leukemic differentiation. *Cancer Cell*. 2021;39(7):958—972.e8.
48. Yankova E, Blackaby W, Albertella M, et al. Small-molecule inhibition of METTL3 as a strategy against myeloid leukaemia. *Nature*. 2021;593(7860):597—601.
49. Vu LP, Pickering BF, Cheng Y, et al. The N(6)-methyladenosine (m(6)A)-forming enzyme METTL3 controls myeloid differentiation of normal hematopoietic and leukemia cells. *Nat Med*. 2017;23(11):1369—1376.
50. Weng H, Huang H, Chen J. RNA N (6)-methyladenosine modification in normal and malignant hematopoiesis. *Adv Exp Med Biol*. 2019;1143:75—93.
51. Qing Y, Su R, Chen J. RNA modifications in hematopoietic malignancies: a new research frontier. *Blood*. 2021;138(8):637—648.
52. Li Z, Weng H, Su R, et al. FTO plays an oncogenic role in acute myeloid leukemia as a N6-methyladenosine RNA demethylase. *Cancer Cell*. 2017;31(1):127—141.
53. Vu LP, Pickering BF, Cheng Y, et al. The N6-methyladenosine (m6A)-forming enzyme METTL3 controls myeloid differentiation of normal hematopoietic and leukemia cells. *Nat Med*. 2017;23(11):1369—1376.
54. Barbieri I, Tzelepis K, Pandolfini L, et al. Promoter-bound METTL3 maintains myeloid leukaemia by m(6)A-dependent translation control. *Nature*. 2017;552(7683):126—131.
55. Huang Y, Su R, Sheng Y, et al. Small-molecule targeting of oncogenic FTO demethylase in acute myeloid leukemia. *Cancer Cell*. 2019;35:677—691.
56. Wang J, Li Y, Wang P, et al. Leukemogenic chromatin alterations promote AML leukemia stem cells via a KDM4C-ALKBH5-AXL signaling Axis. *Cell Stem Cell*. 2020;27(1):81—97.e8.
57. Weng H, Huang F, Yu Z, et al. The m(6)A reader IGF2BP2 regulates glutamine metabolism and represents a therapeutic target in acute myeloid leukemia. *Cancer Cell*. 2022;40:1—17.
58. Li Z, Qian P, Shao W, et al. Suppression of m(6)A reader Ythdf2 promotes hematopoietic stem cell expansion. *Cell Res*. 2018;28(9):904—917.
59. Wang H, Zuo H, Liu J, et al. Loss of YTHDF2-mediated m(6)A-dependent mRNA clearance facilitates hematopoietic stem cell regeneration. *Cell Res*. 2018;28(10):1035—1038.
60. Chen Z, Shao YL, Wang LL, et al. YTHDF2 is a potential target of AML1/ETO-HIF1alpha loop-mediated cell proliferation in t(8;21) AML. *Oncogene*. 2021;40(22):3786—3798.
61. Zhang L, Zhao X, Wang J, et al. METTL3 suppresses neuropathic pain via modulating N6-methyladenosine-dependent primary miR-150 processing. *Cell Death Dis*. 2022;8(1):80.
62. Lechman ER, Gentner B, van Galen P, et al. Attenuation of miR-126 activity expands HSC in vivo without exhaustion. *Cell Stem Cell*. 2012;11(6):799—811.
63. de Leeuw DC, Denkers F, Olthof MC, et al. Attenuation of microRNA-126 expression that drives CD34+38- stem/progenitor cells in acute myeloid leukemia leads to tumor eradication. *Cancer Res*. 2014;74(7):2094—2105.
64. Lechman ER, Gentner B, Ng SWK, et al. miR-126 regulates distinct self-renewal outcomes in normal and malignant hematopoietic stem cells. *Cancer Cell*. 2016;29(4):602—606.
65. Li Z, Chen P, Su R, et al. Overexpression and knockout of miR-126 both promote leukemogenesis. *Blood*. 2015;126(17):2005—2015.
66. Zhang L, Nguyen LXT, Chen YC, et al. Targeting miR-126 in inv(16) acute myeloid leukemia inhibits leukemia development and leukemia stem cell maintenance. *Nat Commun*. 2021;12(1):6154.
67. Zhang B, Nguyen LXT, Zhao D, et al. Treatment-induced arteriolar revascularization and miR-126 enhancement in bone marrow niche protect leukemic stem cells in AML. *J Hematol Oncol*. 2021;14(1):122.
68. Bagger FO, Kinalis S, Rapin N. BloodSpot: a database of healthy and malignant haematopoiesis updated with purified and single cell mRNA sequencing profiles. *Nucleic Acids Res*. 2019;47(D1):D881—D885.
69. Haferlach T, Kohlmann A, Wieczorek L, et al. Clinical utility of microarray-based gene expression profiling in the diagnosis and subclassification of leukemia: report from the International Microarray Innovations in Leukemia Study Group. *J Clin Oncol*. 2010;28(15):2529—2537.
70. Caicedo HH, Hashimoto DA, Caicedo JC, Pentland A, Pisano GP. Overcoming barriers to early disease intervention. *Nat Biotechnol*. 2020;38(6):669—673.
71. Li JH, Liu S, Zhou H, Qu LH, Yang JH. starBase v2.0: decoding miRNA-ceRNA, miRNA-ncRNA and protein-RNA interaction networks from large-scale CLIP-Seq data. *Nucleic Acids Res*. 2014;42(Database issue):D92—D97.
72. Jiang X, Huang H, Li Z, et al. Blockade of miR-150 maturation by MLL-fusion/MYC/LIN-28 is required for MLL-associated leukemia. *Cancer Cell*. 2012;22(4):524—535.
73. Qing Y, Dong L, Gao L, et al. R-2-hydroxyglutarate attenuates aerobic glycolysis in leukemia by targeting the FTO/-m6A/PFKP/LDHB axis. *Mol Cell*. 2021;81(5):922—939.e9.
74. Ma S, Yan J, Barr T, et al. The RNA m6A reader YTHDF2 controls NK cell antitumor and antiviral immunity. *J Exp Med*. 2021;218(8):e20210279.
75. Kozomara A, Birgaoanu M, Griffiths-Jones S. miRBase: from microRNA sequences to function. *Nucleic Acids Res*. 2019;47(D1):D155—D162.

76. Forero DA, Gonzalez-Giraldo Y, Castro-Vega LJ, Barreto GE. qPCR-based methods for expression analysis of miRNAs. *Biotechniques*. 2019;67(4):192—199.
77. Schmittgen TD, Jiang J, Liu Q, Yang L. A high-throughput method to monitor the expression of microRNA precursors. *Nucleic Acids Res*. 2004;32(4):e43.
78. Su R, Dong L, Li Y, et al. Targeting FTO suppresses cancer stem cell maintenance and immune evasion. *Cancer Cell*. 2020; 38(1):79—96.e11.
79. Han L, Dong L, Leung K, et al. METTL16 drives leukemogenesis and leukemia stem cell self-renewal by reprogramming BCAA metabolism. *Cell Stem Cell*. 2023;30(1):52—68.e13.
80. Krivtsov AV, Twomey D, Feng Z, et al. Transformation from committed progenitor to leukaemia stem cell initiated by MLL-AF9. *Nature*. 2006;442(7104):818—822.
81. Wang Y, Krivtsov AV, Sinha AU, et al. The Wnt/beta-catenin pathway is required for the development of leukemia stem cells in AML. *Science*. 2010;327(5973):1650—1653.
82. Cusan M, Cai SF, Mohammad HP, et al. LSD1 inhibition exerts its antileukemic effect by recommissioning PU.1- and C/EBPalpha-dependent enhancers in AML. *Blood*. 2018; 131(15):1730—1742.
83. Fong CY, Gilan O, Lam EY, et al. BET inhibitor resistance emerges from leukaemia stem cells. *Nature*. 2015;525(7570): 538—542.
84. Rathert P, Roth M, Neumann T, et al. Transcriptional plasticity promotes primary and acquired resistance to BET inhibition. *Nature*. 2015;525(7570):543—547.
85. Ye M, Zhang H, Yang H, et al. Hematopoietic differentiation is required for initiation of acute myeloid leukemia. *Cell Stem Cell*. 2015;17(5):611—623.
86. Greenblatt SM, Man N, Hamard PJ, et al. CARM1 is essential for myeloid leukemogenesis but dispensable for normal hematopoiesis. *Cancer Cell*. 2018;34(5):868.
87. Jiang X, Huang H, Li Z, et al. Blockade of miR-150 maturation by MLL-fusion/MYC/LIN-28 is required for MLL-associated leukemia. *Cancer Cell*. 2012;22(4):524—535.
88. Chen P, Price C, Li Z, et al. miR-9 is an essential oncogenic microRNA specifically overexpressed in mixed lineage leukemia-rearranged leukemia. *Proc Natl Acad Sci U S A*. 2013; 110(28):11511—11516.
89. Jiang X, Hu C, Arnovitz S, et al. miR-22 has a potent anti-tumor role with therapeutic potential in acute myeloid leukemia. *Nat Commun*. 2016;7:11452.
90. Jiang X, Huang H, Li Z, et al. miR-495 is a tumor-suppressor microRNA down-regulated in MLL-rearranged leukemia. *Proc Natl Acad Sci USA*. 2012;109(47):19397—19402.
91. Weng H, Lal K, Yang FF, Chen J. The pathological role and prognostic impact of miR-181 in acute myeloid leukemia. *Cancer Genet*. 2015;208(5):225—229.
92. Youn JY, Dunham WH, Hong SJ, et al. High-density proximity mapping reveals the subcellular organization of mRNA-associated granules and bodies. *Mol Cell*. 2018;69(3): 517—532.e11.
93. Döhner H, Longo DL, Weisdorf DJ, Bloomfield CD. Acute myeloid leukemia. *N Engl J Med*. 2015;373(12):1136—1152.
94. Burnett A, Wetzler M, Lowenberg B. Therapeutic advances in acute myeloid leukemia. *J Clin Oncol*. 2011;29(5):487—494.
95. Velasco-Hernandez T, Sawen P, Bryder D, Cammenga J. Potential pitfalls of the mx1-cre system: implications for experimental modeling of normal and malignant hematopoiesis. *Stem Cell Rep*. 2016;7(1):11—18.
96. Healy FM, Dahal LN, Jones JRE, Floisand Y, Woolley JF. Recent progress in interferon therapy for myeloid malignancies. *Front Oncol*. 2021;11:769628.
97. Yilmaz OH, Morrison SJ. The PI-3kinase pathway in hematopoietic stem cells and leukemia-initiating cells: a mechanistic difference between normal and cancer stem cells. *Blood Cells Mol Dis*. 2008;41(1):73—76.
98. Erson-Bensan AE, Begik O. m6A Modification and Implications for microRNAs. *MicroRNA*. 2017;6(2):97—101.
99. Wang H, Deng Q, Lv Z, et al. N6-methyladenosine induced miR-143-3p promotes the brain metastasis of lung cancer via regulation of VASH1. *Mol Cancer*. 2019;18(1):181.
100. Ma JZ, Yang F, Zhou CC, et al. METTL14 suppresses the metastatic potential of hepatocellular carcinoma by modulating N(6) -methyladenosine-dependent primary MicroRNA processing. *Hepatology*. 2017;65(2):529—543.
101. Han J, Wang JZ, Yang X, et al. METTL3 promote tumor proliferation of bladder cancer by accelerating pri-miR221/222 maturation in m6A-dependent manner. *Mol Cancer*. 2019; 18(1):110.
102. Chen P, Li S, Zhang K, et al. N(6)-methyladenosine demethylase ALKBH5 suppresses malignancy of esophageal cancer by regulating microRNA biogenesis and RAI1 expression. *Oncogene*. 2021;40(37):5600—5612.
103. Du H, Zhao Y, He J, et al. YTHDF2 destabilizes m(6)A-containing RNA through direct recruitment of the CCR4-NOT deadenylase complex. *Nat Commun*. 2016;7:12626.
104. Liu X, Jin DY, McManus MT, Mourelatos Z. Precursor microRNA-programmed silencing complex assembly pathways in mammals. *Mol Cell*. 2012;46(4):507—517.
105. Diederichs S, Haber DA. Dual role for argonautes in microRNA processing and posttranscriptional regulation of microRNA expression. *Cell*. 2007;131(6):1097—1108.
106. Jin D, Guo J, Wu Y, et al. m(6)A demethylase ALKBH5 inhibits tumor growth and metastasis by reducing YTHDFs-mediated YAP expression and inhibiting miR-107/LATS2-mediated YAP activity in NSCLC. *Mol Cancer*. 2020;19(1):40.
107. Frohn A, Eberl HC, Stohr J, et al. Dicer-dependent and -independent Argonaute2 protein interaction networks in mammalian cells. *Mol Cell Proteomics*. 2012;11(11): 1442—1456.